Transport critical current of aligned polycrystalline $Y_1Ba_2Cu_3O_{7-\delta}$ and evidence for a nonweak-linked component of intergranular current conduction

J. W. Ekin
National Institute of Standards and Technology, Electromagnetic Technology Division, Boulder, Colorado 80303

H. R. Hart, Jr. and A. R. Gaddipati[a)]
GE Corporate Research and Development, Schenectady, New York 12301

(Received 31 October 1989; accepted for publication 22 June 1990)

A study of grain alignment and its effect on the dc transport critical current in fine-grained bulk $Y_1Ba_2Cu_3O_{7-\delta}$ is reported in magnetic fields from 10^{-4} T to 26 T. Two features distinguish the critical current density J_c of aligned bulk $Y_1Ba_2Cu_3O_{7-\delta}$ from unaligned material. First, the effective critical field where the intergranular J_c approaches zero is about four times higher (30 T) for aligned samples with field parallel to the *a*, *b* planes, than it is for polycrystalline unaligned samples (7 T). Second, the nearly field independent plateau value of J_c between 10 mT and 1 T is one to two orders of magnitude higher than typical plateau values of J_c in unaligned bulk-sintered $Y_1Ba_2Cu_3O_{7-\delta}$, for field parallel to the *a*, *b* planes. A low-field (<10 mT) weak-link decrease in J_c with magnetic field is still observed, but it is much smaller than for unaligned material. These data clearly demonstrate that alignment alone significantly reduces the *weak-link* problem in fine-grained polycrystalline samples with low-aspect-ratio (4:1) grains (unlike melt-grown samples where there has been some ambiguity as to the relative importance of alignment versus large grain growth). Furthermore, the results provide strong evidence that there are two parallel components of *intergranular* current conduction, one consisting of weak-linked material, the other behaving like intrinsic intragranular material that is not weak-linked. A comparison with unaligned $Y_1Ba_2Cu_3O_{7-\delta}$ indicates that the volume fraction of such nonweak-linked material is significantly enhanced by grain alignment, but still only 0.01%–0.1% of the grain boundary area. Field-cooled and force-free J_c data are also presented, along with detailed measurements of the shapes of the voltage-current characteristics.

I. INTRODUCTION

A. Background

Recent data on the transport critical current density J_c of bulk sintered Y-, Bi-, and Tl-based high-T_c superconductors over a wide magnetic field range have shown a double-step characteristic, where J_c decreases rapidly with an approximate $B^{-3/2}$ power dependence on the magnetic field B ($\equiv\mu_0 H$) starting at about 10^{-4} T and ending between 10^{-3} and 10^{-2} T, depending on the sample.[1] Above this low-field regime there is a wide field range where J_c is relatively independent of magnetic field. At still higher fields, J_c eventually decreasing to zero, above ~5 T–7 T for Y-based bulk-sintered materials and above ~2 T for Bi- and Tl-based bulk-sintered materials, at 76 K. The low field ($<10^{-2}$ T) drop is fit well by a theory of Josephson weak links occurring at the grain boundaries; this was interpreted as evidence for weak-link decoupling of the grain boundaries in this low-field regime. However, such a weak-link model cannot explain the relatively field independent behavior of J_c at higher fields ($>10^{-2}$ T), up to over 1 T.

This field-independent regime for the intergranular J_c resembles the nearly field-independent J_c in single crystalline samples, and consequently it was speculated that this higher field behavior was the result of a second component of nonweak-linked intergranular conduction within the bulk superconductor that is not decoupled by the magnetic field.[1,2] This second component of intergranular conduction is usually not observable at very low fields in materials with a large fraction of weak-linked material because it is masked by the much greater conduction of the (not yet decoupled) weak-linked material. More recent transport data on an isolated single weak-linked grain boundary in thin films[3,4] suggests that large variations in J_c occur along a single grain boundary and, thus, this second component could arise from regions of strong conduction within each grain boundary (e.g., microbridges).[5]

The resemblance of this second nonweak-linked component to the *intra*granular critical current is further evidenced by the close correlation between the value of the field at which the transport J_c of *unaligned* polycrystalline samples[1] decreases to zero at high fields and with the effective critical field $H_{c2}^*(\|c\text{ axis})$ measured for transport conduction in single crystalline samples[6–9] and samples with decoupled, aligned grains in epoxy[10,11] [where $H_{c2}^*(\|c\text{ axis})$ is the value of H_{c2}^* in single crystalline sam-

[a)]Now at the Knolls Atomic Power Laboratory, Schenectady, NY.

 0021-8979/90/172285-11$02.40

ples when the magnetic field is oriented along the unfavorable c-axis direction].

B. Aligned $YBa_2Cu_3O_7$

An investigation of the transport J_c in *aligned* materials provides a good test of this model. If such a second component of *inter*granular conduction exists that is not weak-linked, but behaves instead like the *intra*granular J_c, then it would be expected to extend to much higher fields before being suppressed to zero, for field along the a, b axes in aligned polycrystalline materials. It would also be expected to exhibit the same anisotropic flux-flow characteristics observed in single-crystalline samples. Thus, to test this hypothesis, extensive dc transport J_c measurements were made on polycrystalline bulk superconductors with grains that were *both aligned and electrically coupled* at high fields. In addition to the high-field properties, it was also of interest to see if grain alignment had any effect on the weak-link nature of the transport J_c at low fields. Consequently a series of measurements were carried out on the dc transport J_c of these aligned, coupled materials over a very wide magnetic field range from 10^{-4} to 26 T.

Our approach[12] to the alignment of the grains was based on the discovery by Farrell and his co-workers[13] that single-crystal particles of $Y_1Ba_2Cu_3O_{7-\delta}$ (YBCO) could be aligned at room temperature by the application of a 9.4 T magnetic field, with the alignment caused by the anisotropy in the paramagnetic susceptibility. In their experiment, the particles were suspended in epoxy at a 27% volume loading. In our experiments the sample preparation is unique in that the magnetic alignment was carried out in a manner that allowed the sintering of an aligned bar, yielding electrically connected grains and a conducting specimen.[12]

The first two sections of this article describe the magnetic alignment technique used to fabricate these YBCO samples and the degree of alignment obtained as measured by x-ray and neutron diffraction. The next section describes the technique used to measure the dc transport J_c. Results of J_c measurements obtained continuously over five orders of magnitude of magnetic field, at both liquid-nitrogen and liquid-helium temperatures, are then presented. In making these measurements, we oriented the magnetic field both perpendicular and parallel to the a,b (Cu-O) planes, with transport current applied along the a,b planes. Measurements are also given for the force-free J_c, wherein the magnetic field is oriented parallel to the applied transport current.

The main result of this work is the demonstration of the significant improvement in the *intergranular* J_c that accompanies alignment, even in fine-grained bulk sintered samples with low-aspect-ratio (4:1) grains. The data clearly demonstrate for the first time that alignment reduces the *weak-link* problem in polycrystalline samples with many (500–1000) grain boundaries between the measurement voltage taps.

Five features of these data are discussed in detail: the evidence for nonweak-linked transgranular supercurrents, the close correspondence between the magnetic-field dependence of J_c and the sharpness of the superconducting transition in the voltage-current characteristics, a significant rise or peak ($\sim$100% increase) in the J_c-vs-B characteristic for B parallel to the Cu-O planes, an enhancement of the weak-link decoupling field compared with unaligned samples, and an increase in the intergranular J_c and H_{c2}^* when temperature is reduced to liquid-helium temperatures.

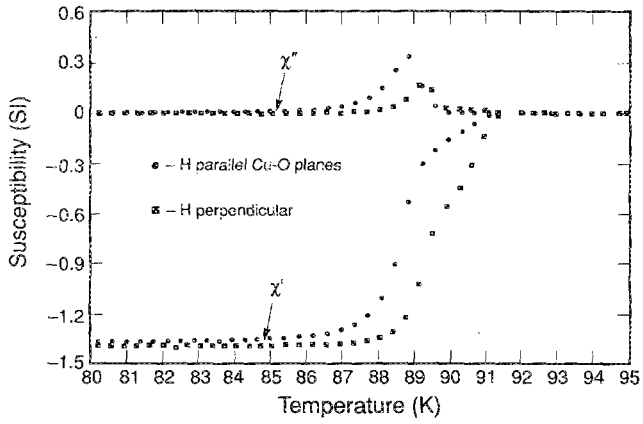

FIG. 1. ac susceptibility vs temperature measured at 1 mT for two samples cut for transport J_c measurements with field parallel (○) and perpendicular (□) to the a,b planes.

II. SAMPLE PREPARATION

The samples were prepared from powders of $YBa_2Cu_3O_{7-\delta}$ obtained by multiple reaction and grinding of high-purity Y_2O_3, $BaCO_3$, and CuO.[14] X-ray diffraction of the powders showed them to be x-ray phase pure. The powders (5-μm volume-weighted average diameter) were suspended in heptane plus a deflocculant, vibromilled for 30 min, and poured into an alumina boat in the 4-T magnetic field of a medical imaging magnet. The suspension was left in the magnetic field for approximately 12 h, during which time the particles aligned and settled, and the heptane evaporated and left a dry cake. The dry cake was removed from the magnet, sintered in flowing oxygen for 10 h at 950 °C, and cooled to room temperature at a rate of 20 °C/h. At no point was the material compacted by the application of pressure. The resulting block (about $9\times3.5\times$ 0.7 cm) was cut into samples for J_c testing using a diamond saw without cutting fluid. The J_c samples had cross-sections approximately 1 mm$\times$3 mm, and were about 15 mm long. The critical temperature of the sample was found by ac susceptibility to have an onset at 91.5 K and a transition midpoint at about 89 K in a magnetic field of 1 mT (see Fig. 1).

III. SAMPLE CHARACTERIZATION

The samples were characterized initially by x-ray diffraction, light microscopy, transmission electron microscopy, and magnetic hysteresis measurements.[12,15] The results are briefly summarized here. The x-ray θ-2θ

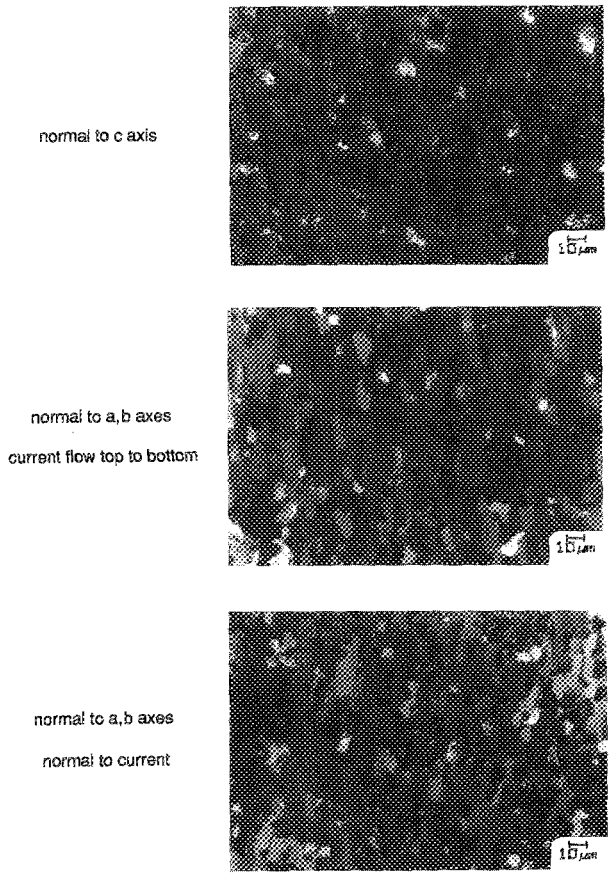

FIG. 2. Micrograph of sample surface showing grain-surfaces (a) normal to c-axis, (b) normal to a and b axes (parallel to current direction), and (c) normal to a and b axes (perpendicular to current direction).

diffraction patterns were consistent with complete alignment, but appreciable misalignment can go undetected in such a scan. For this reason x-ray rocking curves were obtained using the (005) reflection; the full-width-at-half-maximum was 12°–15°. X-ray pole figure measurements[16] yielded results in agreement with the rocking-curve results. Since the effective penetration depth of the x-ray beam is 5–20 μm, only the surface of the sample is probed in the x-ray diffraction, rocking angle, and pole figure studies. Neutron diffraction, on the other hand, allows a measurement of the alignment in the bulk of the sample. Such a measurement[17] yielded an angular full-width-at-half-maximum of 19°. Thus, significant alignment was obtained, but the residual misalignment is far greater than that of epitaxial thin films.

Light micrographs[15] likewise indicate significant but incomplete alignment, as shown in Fig. 2. The grains are in the form of platelets with thicknesses of about 5 μm and face dimensions of about 20×20 μm. The c-axis is perpendicular to the platelet. There are substantial regions devoid of well-formed grains; these regions occupy roughly one-third of the volume of the sample. Sample density is 75% of the theoretical value for YBCO.

Measurements of electrical resistivity at room temperature yielded an anisotropy ratio of 14:1, typically 450 $\mu\Omega$ cm in the nominal a,b-direction and 6.3 mΩ cm in the nominal c-direction.

IV. EXPERIMENT

Low resistivity current contacts were made to the samples by a low-temperature process wherein the sample surface was first sputter etched, followed by sputter deposition of 6-μm-thick Ag contact pads.[18] The superconductor and Ag pads were then oxygen annealed at an intermediate temperature of 550 °C for 1 h.[19–21] Two small copper bus bars were soldered to the Ag contact pads with an indium-alloy solder. The resulting contact resistivities were in the range from 6×10^{-8} to 8×10^{-7} Ω cm^2 at 76 K and 3×10^{-8} to 4×10^{-8} Ω cm^2 at 4 K.

Samples were tested with the transport current applied along the a,b plane, and with magnetic field either perpendicular or parallel to the a,b plane (and normal to the current, unless otherwise specified). A four-terminal dc method was used to determine the transport critical-current density. Voltage taps were ultrasonically soldered to the sample surface using an indium alloy solder, since very low contact resistance is not needed for voltage detection. The distance between the two voltage taps was 5.7 mm. The dc voltage detection limit of our apparatus was about 3 nV.

The critical-current density was determined using a 1 μV/mm offset criterion in order to minimize the sensitivity of J_c to the criterion level.[22] The offset criterion consists of taking the tangent to the E-J curve at a given electric-field level, E_c. The critical current is defined as the current where this tangent extrapolates to zero electric field. The offset criterion defines an intrinsic superconducting J_c that goes to zero where the E-J characteristic of a material becomes completely ohmic, unlike conventional criteria where the defined J_c is the result of an arbitrary interaction between criterion level and normal-state conduction. Essentially, the offset criterion is similar to the electric-field criterion, but it eliminates the normal-conduction component inherent in the electric-field criterion, and much of the arbitrariness associated with the criterion level at high magnetic fields near the upper critical field.

The measurements were carried out using a magnet designed to allow continuous variation of the applied magnetic field over five orders of magnitude from 10^{-4} to 10 T in the same cryostat without thermally cycling the sample. Measurements were carried out both in liquid nitrogen at 76 K and in liquid helium at 4 K (the temperatures are slightly lower than those typically quoted because the measurements were made about 1600 m above sea level). The magnetic field was ramped monotonically (without overshoot) to the desired measurement field.

For magnetic field applied parallel to the a,b planes at fields between 0.02 and 5 T, the critical current decreased slowly with time over a period of several minutes if the transport current was left applied to the sample at a value near the critical current. Data were obtained after J_c approached an asymptotic value and the drift had slowed to a negligible level ($<0.5\%$/min). The largest total decrease was about 5% and occurred at about 0.1 T.

The critical current was measured not only in the usual way with field perpendicular to the applied transport current, but also in the "force-free" configuration with field

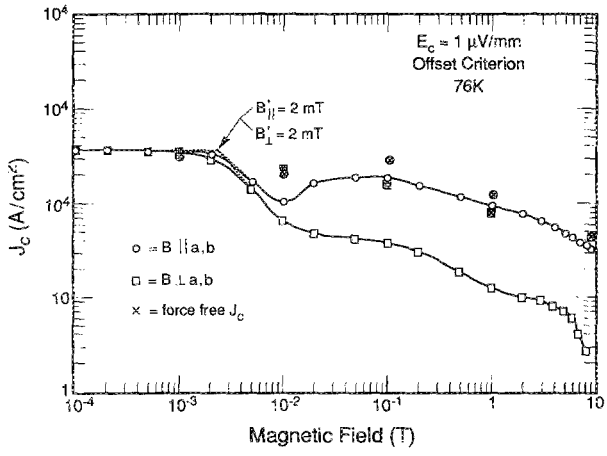

FIG. 3. Intergranular transport J_c (B) characteristics of aligned $Y_1Ba_2Cu_3O_{7-\delta}$ for two magnetic-field orientations at liquid-nitrogen temperature. Force-free J_c values (parallel current and field) are shown by symbols filled with an $\times$. Note the significant enhancement in the transport critical field and plateau J_c value for magnetic field paralle to the a,b planes.

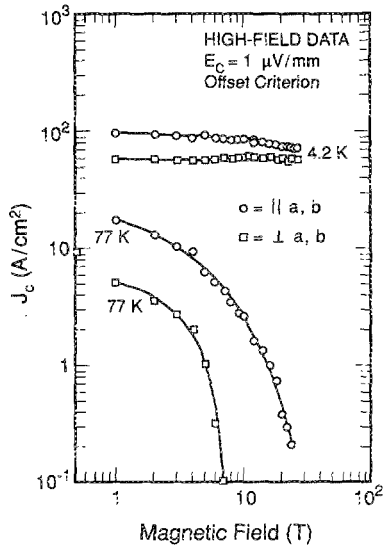

FIG. 4 High-field transport J_c (B) characteristics of aligned $Y_1Ba_2Cu_3O_{7-\delta}$ for two magnetic field orientations at 77 and 4.2 K.

parallel to the applied transport current in the a,b plane. This was done by rotating the sample (at constant field) in the bore of a radial access magnet without removal of the sample from the cryostat (to avoid thermal cycling). After rotation back to the original (perpendicular) field orientation, the critical-current density was slightly ($<15\%$) different because of trapped flux effects from the field-angle rotation. To eliminate this effect, the magnetic field was cycled to zero after every such rotation and then raised back to the original value, where J_c was observed to reproduce the value originally measured before field rotation.

A special procedure was used to assess the difference between flux-exclusion and flux-expulsion effects on J_c. The sample was cooled *in field* from just above T_c to liquid-nitrogen temperature and then J_c was measured in this field-cooled state. This procedure was repeated at each level of applied magnetic field in order to obtain a *field-cooled* $J_c(B)$ curve to compare with the more usual zero-field-cooled data.

For these field-cooled tests, the voltage would sometimes jump to a higher level and stay there when the current approached J_c. The largest jumps were about 1 μV and occurred at about 0.1 T, diminishing to about half this size at 1 T. They occurred only when the applied magnetic field was oriented perpendicular to the a,b planes, and not for field applied parallel to the a,b planes. J_c decreased by less than 3% for the largest voltage jumps.

V. RESULTS

A. $J_c(B)$ at 76 K

Figure 3 presents the dc transport critical-current density J_c along the a,b planes as a function of magnetic field applied parallel and perpendicular to the a,b-axes, at liquid-nitrogen temperature. The open symbols present the data measured for mutually perpendicular current and magnetic field; $\times$-filled symbols denote the force-free case where the applied magnetic field has been rotated parallel to the current direction from either the $B\|a,b$ direction or $B\perp a,b$ direction.

The data for field *parallel* to the a,b plane (circles in Fig. 3) show a deviation from the double-step characteristic that is generally observed in bulk unaligned polycrystalline high-T_c superconductors.[1] The first low-field step is observed, similar to the unaligned case, but then, in contrast to the unaligned case, this is followed by a large rise in J_c at intermediate fields between 10 and 50 mT. This rise appears slight on the log scale of Fig. 3, but actually corresponds to a 100% rise in J_c from its low point at 10 mT. Such a peak or rise in the $J_c(B)$ curve has been consistently observed for field parallel to the a,b plane in repeated measurements.

In the region between 10^{-2} and 1 T, the transport J_c for B parallel to the a,b planes is over 100 A/cm^2, which is one to two orders of magnitude higher than the plateau value of J_c for typical unaligned YBCO samples. At 10 T, the transport J_c was still over 30 A/cm^2. This is one of the highest values of transport J_c(10 T) for *bulk-sintered* YBCO.

In addition to the much higher plateau value of J_c, another difference compared with unaligned YBCO samples is that the high-field drop in J_c is shifted to a significantly higher magnetic field when the field is parallel to the a,b planes. For unaligned samples, the effective critical field for transport conduction B^*_{c2} $(T=76$ K), $(B^*_{c2}\equiv\mu_0 H^*_{c2})$, is less than 7 T.[1] On the other hand, for these aligned samples, B^*_{c2} was so high in the parallel orientation that we had to perform a separate measurement using a high-field hybrid magnet to measure it. The results are shown in Fig. 4. (The plateau value of J_c in this separate test, performed about 4 months after the low-field measurements, is lower, indicating variability of the plateau J_c value in these samples with time.) The data in Fig. 4 show that $B^*_{c2}(T=77$ K) for this field orientation *approaches 30 T*, more than a three fold increase compared with the unaligned case.

Figure 3 also shows the corresponding J_c-vs-B characteristic when the magnetic field is applied *perpendicular* to

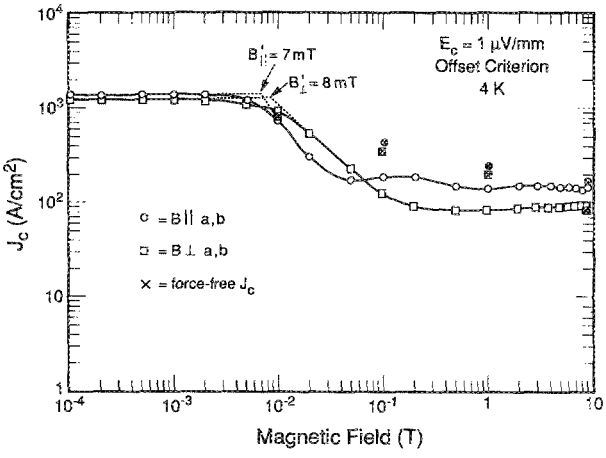

FIG. 5. Same as Fig. 3 at liquid-helium temperature.

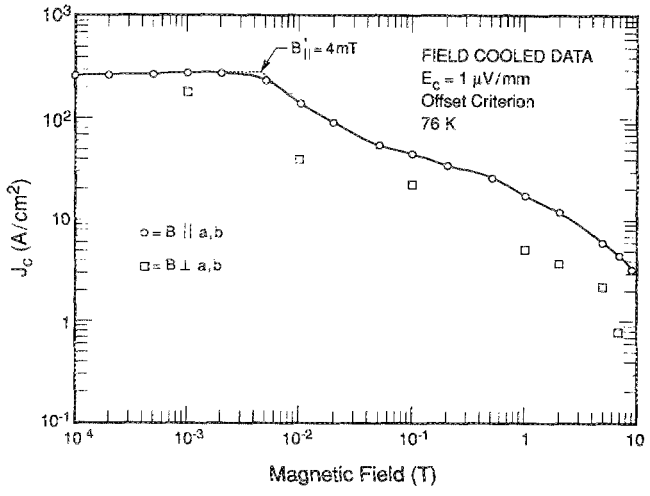

FIG. 6. Transport J_c (B) characteristics of aligned $Y_1Ba_2Cu_3O_{7-\delta}$ obtained by *cooling the sample in the magnetic field* at each data point.

the Cu-O planes (square symbols). Here the data resemble much more closely the two-step characteristic of unaligned samples.[1] The low-field step is nearly the same as for the parallel case, but there is no rise in J_c at intermediate fields, and B^*_{c2} is only about 9 T, similar to the unaligned case. Also the plateau value of J_c for field perpendicular to the a,b plane is about 5 times lower than for field parallel to the a,b plane. This is similar to the anisotropy observed at 77 K in the transport J_c of high-quality epitaxial YBCO thin films.

B. Force-free J_c

The change in J_c when field is rotated parallel to the current, that is the "force-free" J_c, is shown by ×-filled symbols in Fig. 3. The force-free J_c shows no enhancement over the usual Lorentz-force J_c in the low-field regime and a 50%–100% enhancement at intermediate magnetic fields (10^{-2}–1 T). This is similar to the enhancement of the force-free J_c above the Lorentz-force J_c in the unaligned case.[2,3] There is also a rise in the force-free J_c data in Fig. 3 at intermediate fields between 10 and 100 mT for field parallel to the a,b planes, similar to the $J_c(B)$ characteristic for the usual Lorentz-force case.

C. $J_c(B)$ at 4 K

Figure 5 shows the corresponding J_c-vs-B characteristics at lower temperature, obtained at 4 K in liquid helium. J_c is enhanced by a factor of a little more than 3, as is the decoupling magnetic field where the first drop in J_c occurs. A small 20% peak in J_c after the first drop still is observable for the parallel-field case and not for the perpendicular-field case, although it is much smaller than at 76 K only ~20% instead of ~100%. The high-field measurements at 4 K plotted in Fig. 5 show no significant decrease in J_c at fields up to the limit of the measurement (27 T), indicating a significant enhancement in the effective upper critical field at this low temperature.

D. Field-cooled J_c

Figure 6 shows the transport J_c measured on the same sample in a separate experiment where the data were obtained by placing the sample in the measuring field in its normal state just above T_c and then *cooling to 76 K in field*. This was repeated at each measuring field. The field-cooled transport J_c data obtained in this manner show a low-field step which starts at a decoupling field that is twice as large as for the usual zero-field cooled data (4 mT in Fig. 6 vs 2 mT in Fig. 3). There is no significant peak in J_c between 10 and 50 mT, unlike the zero-field-cooled case. The data still show residual characteristics of the double-step pattern, with a gradual leveling in the $J_c(B)$ curve starting in the 10^{-2} T range, followed by an increasing rate of fall at higher fields.

E. Transition parameter $n[\equiv d(\ln V)/d(\ln I)]$

For unaligned polycrystalline samples, a plot of ln V vs ln I is remarkably linear over the entire range of measurement, from about 1 μV/cm to 100 μV/cm.[1] Thus, the V-I characteristic for the unaligned polycrystalline case is a nearly pure power law dependence, similar to conventional strongly pinned superconductors.

For these aligned polycrystalline superconductors, however, the voltage rises with current less rapidly than a pure power law. An example of the V-I curves is shown in Fig. 7 for the case where B is parallel to the a,b planes at 76 K. As seen in Fig. 7, the logarithmic V-I characteristic has negative curvature, $d^2 \ln V/d^2 \ln I < 0$. A negative curvature of the ln V vs ln I curve, similar to that in Fig. 7, was observed at both 76 and 4 K, and for both field orientations (parallel and perpendicular to the a,b planes).

The slope of the ln V vs ln I curve, n, has been determined at an electric field of 10 μV/cm for each of the cases studied and a typical set of results are plotted as a function of magnetic field in Figs. 8 and 9. Here n is defined by the relation $E \propto J^n$ [or, equivalently, $V \propto I^n$ or $n \equiv d(\ln V)/d(\ln I)$]. The higher the value of n, the sharper the take-off

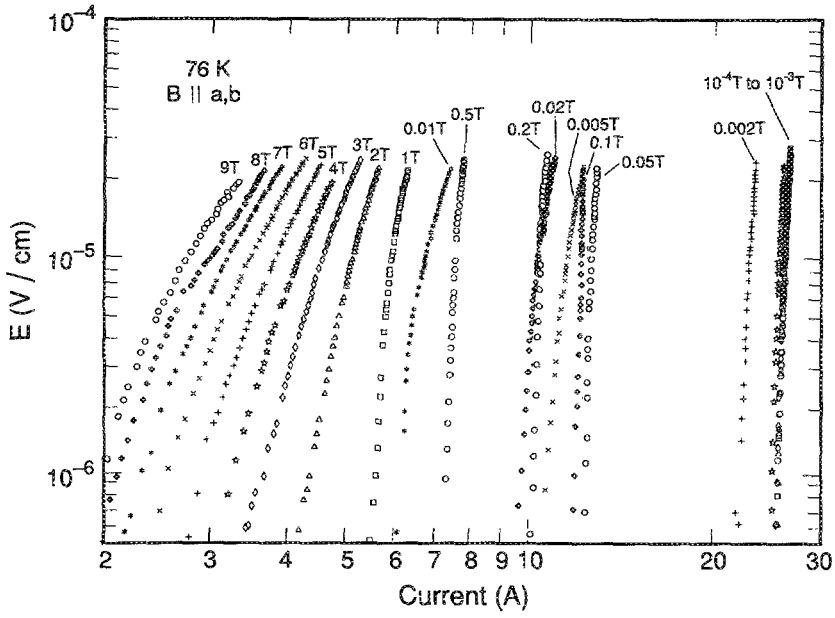

FIG. 7. Logarithmic plot of electric field versus current at 76 K at different magnetic fields for the case of B parallel to the a,b planes. The slight negative curvature is typical at both 76 and 4 K, and for both field orientations ($B\|a,b$ planes and $B\perp a,b$ planes), indicating less than a pure power law dependence in all cases.

in the V-I characteristic at the critical current. Figures 8 and 9 show that, at high fields ($>10^{-2}$ T), n is much higher for field oriented parallel to the a,b planes than for field perpendicular to the a,b planes. There is also a significant peak in the $n(B)$ curve for B parallel to the a,b planes at 76 K, similar to the $J_c(B)$ curve for this orientation shown in Fig. 3. Values of n are fairly high in the plateau regime [~ 20 and ~ 6 for the parallel and perpendicular geometries in Fig. 8, but in some cases (as shown, for example, in Fig. 7) can be as high as 60 at 76 K in the plateau regime for B parallel to the a,b planes]. This indicates a sharp superconductor-normal transition and a well-defined critical current even at high fields.

At 4 K the shift in the n-vs-B characteristic is similar to the shift in the J_c-vs-B characteristic on cooling from liquid-nitrogen to liquid-helium temperature. The decoupling field is enhanced and the overall magnitude of n is higher. The peak in the n-vs-B curve for field parallel to the a,b planes nearly disappears at 4 K, similar to the large reduction in the $J_c(B)$ peak observed on cooling to 4 K.

VI. DISCUSSION

A. Nonweak-link component of intergranular current conduction

The observation that the transport J_c in these fine-grained superconductors persists to much higher magnetic fields than for unaligned granular superconductors is significant, both practically and fundamentally. As described briefly in the introduction, the double-step behavior of the $J_c(B)$ characteristic in unaligned polycrystalline superconductors has been ascribed to two parallel components of intergranular current conduction, a low field ($B<10^{-2}$ T) component that is dominated by weak-link decoupling at

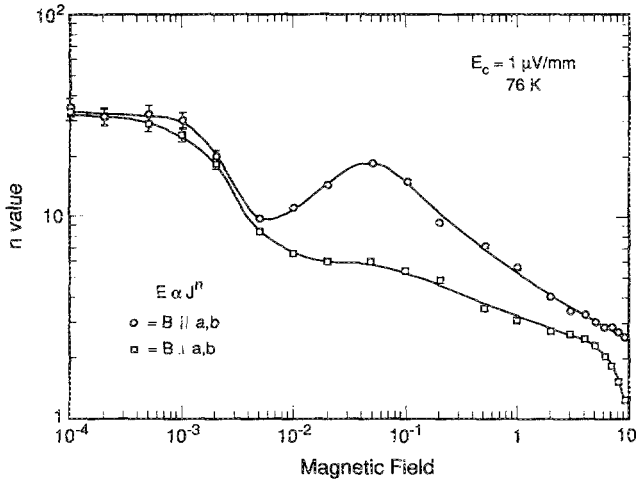

FIG. 8. Transition parameter n as a function of magnetic field for aligned $Y_1Ba_2Cu_3O_{7-\delta}$, measured for two magnetic-field orientations at liquid-nitrogen temperature. The value of n was determined from the defining relation $E\propto J^n$ (or equivalently $V\propto I^n$; $n\equiv d\ln V/d\ln I$) at an electric field $E_c=10$ μV/cm.

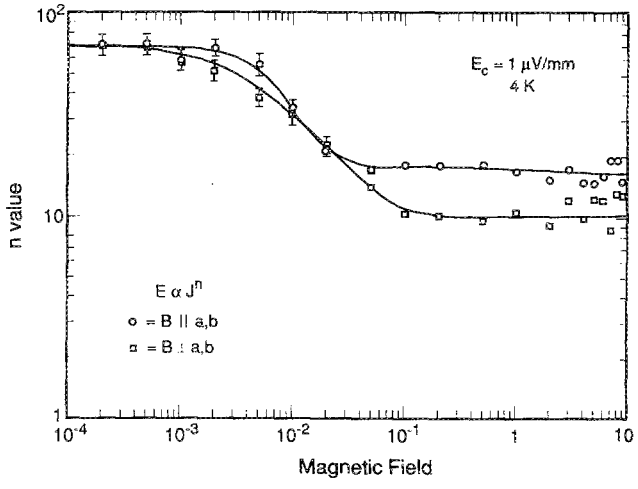

FIG. 9. Same as Fig. 8 at liquid-helium temperature.

the grain boundaries and a high-field ($B > 10^{-2}$ T) component that is conduction tentatively ascribed to a small fraction of remnant paths that are not limited by weak links. The nonweak-linked component of transport J_c that emerges above $\sim 10^{-2}$T is much smaller in polycrystalline samples than in single-crystalline materials, it was speculated, because the nonweak-linked second component occupies only a small fraction of material in polycrystalline samples.

This hypothesis for the existence of a nonweak-linked second component of intergranular conduction was made because of the resemblance of the magnetic-field dependence of J_c in polycrystalline samples above 10^{-2} T to the $J_c(B)$ curve of single-crystalline samples. $J_c(B)$ above 10^{-2} T in both types of materials is nearly field independent until relatively high fields > 1 T. The transport J_c of unaligned polycrystalline samples decreases to zero at about 7 T, at 76 K. This field is very close to the value of $B^*_{c2}(\|c$ axis) measured in single crystalline samples (about 7 T at 77 K); it was argued that the low value of $B^*_{c2}(\|c$ axis) dominates the *unaligned* polycrystalline case because B^*_{c2} is about equal to $B^*_{c2}(\|c$ axis) over a wide range of field angles about the c axis. Thus, the resemblance in field dependence and transport critical field value is striking and led to the speculation that this high field component of *inter*granular transport current was not being dominated by weak links, but by the anisotropic flux-flow characteristic of the *intra*granular J_c.

The data reported here for *aligned* polycrystalline YBCO show a marked contrast to the earlier unaligned data. For field oriented along the a,b planes, the transport J_c at 76 K shown in Figs. 3 and 4 persists to a much higher field of about 30 T. This is very close to the higher value of B^*_{c2} measured in single crystalline samples for field along the a,b direction, constituting strong evidence that the intergranular transport J_c of polycrystalline samples at high fields (> 10 mT) is in fact behaving like the intragranular J_c and that intrinsic nonweak-linked conduction exists in parallel to the low-field weak-linked conduction.

This conclusion is further supported by the fact that the plateau J_c values in Figs. 3 and 4 are larger for magnetic field along the a,b planes, than along the c-axis direction. This observed anisotropy is similar to that measured over the same field range for intragranular YBCO material, as determined from transport $J_c(B)$ studies on epitaxial YBCO films. This suggests the very reasonable hypothesis that the strong-linked material bridging aligned grain boundaries has the same crystalline orientation as the intragranular material on either side of the grain boundary. The temperature dependence of B^*_{c2} is also similar to that in single crystalline YBCO. On cooling to 4 K, the zero-J_c critical field in Figs. 3 and 4 for the aligned fine-grained samples increases to fields well beyond our measurement capability, showing the same intrinsic tendencies observed in transport $J_c(B)$ studies on epitaxial YBCO films.

According to this two-component model, the relatively large magnitude of the plateau J_c also indicates that the fraction of nonweak-linked current conduction is much greater (about two orders of magnitude) for aligned polycrystalline samples than for unaligned samples. That is, alignment greatly enhances the fractional area of nonweak-linked material and hence J_c at practical field levels ($> 10^{-2}$ T).

B. Alternative explanations for the high-field component

An alternative explanation is that the broad J_c plateau region arises from intragranular flux penetration above B_{c1}. That is, suppose there is only the weak-link conduction component; above B_{c1} the flux starts to penetrate into the intragranular material, lowering the flux concentration at the grain boundaries to the extent that the weak-link J_c stops decreasing, even in an increasing applied magnetic field. However, because of the need to overcome the intragranular pinning force, it is difficult to see how this could prevent the flux from rising at the grain boundaries with increasing applied field over several orders of magnitude. Rather, the onset of flux penetration might slow the rate of increase of field at grain boundaries, but not stop it completely over such a wide magnetic-field range (10^{-2} T to over ~ 1 T), which is needed to explain the plateau region of the J_c-vs-B curve if all transport current conduction were weak-linked.

The enhancement in the plateau J_c over that in unaligned polycrystalline samples also cannot be explained simply by an increase in the aspect ratio of the grains. The grain aspect ratio for these samples is only 4, far too small to account for the observed increase in the plateau J_c by one to two orders of magnitude.

It has also been suggested that, instead of strong-linked material, the high-field component arises simply from percolation paths of weak-linked grain boundaries that are aligned exactly perpendicular to the applied magnetic field. That is, for such grain boundaries there is no component of magnetic field threading the weak link barriers and no decoupling of the weak-links. Such a model fails, however, to explain the persistence of J_c to fields over 30 T. This is an enhancement by many orders of magnitude over the usual weak-link decoupling field of a few mT. To achieve such an enhancement in the decoupling field in these samples would require the grain boundaries to be aligned with the magnetic field to within 1 part in 10^4. But the angular spread in the crystal orientation is no better than about 10° (FWHM) in these samples, and closer to 19° as measured by neutron diffraction. Also, this explanation fails to explain why the magnetic field where J_c is suppressed to zero is consistently about 30 T, for field parallel to the a,b planes. If the conduction were controlled by weak links, the zero-J_c field should vary greatly with the geometry of the grain boundaries and not be coincident with the value of $B^*_{c2}(\|a,b$ planes) measured in single-crystalline YBCO or epitaxial-film samples.

On the other hand, the two-component, nonweak-link model described above is at least consistent with all these factors, including the very high value of B^*_{c2} (the effective critical field for transport conduction), the angular anisotropy of B^*_{c2} for aligned grain boundaries, the temperature

dependence of B_{c2}^{*}, the near independence of J_c on magnetic field at fields above ~ 10 mT out to fields near B_{c2}^{*}, and the angular anisotropy of the plateau J_c value.

C. Dependence of the transition parameter, n, on magnetic field

The shape of the n vs B characteristic is also consistent with a change in dissipation mechanism where the strong-linked component becomes dominate (above about 10^{-2} T). The value of n can be associated with the sharpness of the distribution of J_c values in an inhomogeneous superconductor, the higher the value of n, the sharper the J_c distribution.[22] With this interpretation, the n- vs- B characteristics in Figs. 8 and 9 indicate a narrow J_c distribution at low fields followed by considerable broadening around 10^{-2} T where the weak- and strong-link contributions are roughly equal. n then has a remarkable rise (to values as high as 60 at 76 K in some of our samples, such as the data shown in Fig. 7) at fields above 10^{-2} T, consistent with a sharpening of the J_c distribution where the strong-linked component starts to dominate. n then decreases at high fields, consistent with increasing J_c inhomogeneity as B approaches B_{c2}^{*}.

D. Peak in J_c for B parallel to the Cu-O planes

We now turn to the observation of the peak, or rise, in the plateau region of the upper J_c-vs-B curve shown in Fig. 3. This peak is observed for B parallel to the a,b planes, but not for B perpendicular to the a,b planes. The peak is quite large, amounting to a $\sim 100\%$ increase in J_c over the field range from 10 to 20 mT.

Several explanations for the peak are possible. The disappearance of the peak for the field-cooled case (Fig. 6) suggests that the onset of flux penetration into the grain can play a role. In fact, the start of the peak at 76 K occurs slightly above the intragranular lower critical field, $B_{c1}(\|a,b \text{ planes}) = 3$ mT, measured in these samples from magnetization-vs-internal field data at 76 K.[24] The J_c vs B curve is also not reversible in this field regime. The peak is seen only for increasing magnetic field. For decreasing field, the transport J_c monotonically rises without a dip. This irreversibility is also consistent with a B_{c1} effect associated with the onset of flux penetration into the grains.

However, it is difficult to see how this could explain the peak only in terms of a drop in the field at the grain boundary and a resulting rise in the weak-link critical current. For field to penetrate into the grains requires the field at the grain boundaries to *monotonically increase* to overcome the intragranular pinning force, leading to a continuous decrease in the weak-link critical current, not a rise as seen between 10^{-2} T and 10^{-1} T. The possible exception to this would be a grain surface barrier to vortex entry, which disappears at the onset of flux entry allowing flux to rush into the grains, resulting in a decrease in magnetic field within the weak-link grain boundary region.

The peak could also arise simply from an enhancement in the *grain-boundary pinning force*. An enhancement of the pinning force within the grain boundaries or within the aligned strong-linked material could result from the onset of flux penetration into the grains just above B_{c1} or from the change in orientation of magnetic field as the applied field is increased and dominates the self field. For example, the intrinsic intragranular pinning force for magnetic field along the a,b planes is much stronger than the intergranular pinning force. When vortices start to penetrate into the grains on either side of a grain boundary at B_{c1}, they would experience a significant pinning force against motion perpendicular to the Cu-O planes; these pinned vortices, in turn, may well exert an additional pinning force in this direction on the intergranular vortices through a vortex-vortex interaction. Such a mechanism would explain the coincidence of the effect with B_{c1}, as well as be consistent with the peak occurring predominately for B parallel to the a,b planes.

E. Weak-link decoupling field

The rapid drop in J_c at very low magnetic fields has been shown to be explained quantitatively by decoupling of Josephson weak links at grain boundaries in bulk unaligned polycrystalline samples.[25,26] According to this Josephson weak-link model, the decoupling field B_0 for the weak links is given by

$$B_0 = \phi_0/\langle D\rangle 2\lambda, \tag{1}$$

where ϕ_0 is the quantum of flux, λ is the penetration depth, and $\langle D\rangle$ is the average grain size in the direction mutually perpendicular to the applied current and magnetic field. B_0 was shown to be insensitive to the shape and spread of the distribution of grain size.

For the case of these aligned samples, we modify this expression here in order to account for the anisotropy in λ in the grain on either side of the grain boundary:

$$B_0 = \phi_0/\langle D\rangle(\lambda_1 + \lambda_2), \tag{2}$$

where λ_1 is the penetration depth into the grain on one side of the boundary (in a direction perpendicular to the grain boundary plane) and λ_2 is the penetration depth into the grain on the other side. Figure 9 shows a schematic diagram of the geometry.

In order to visualize the decoupling field and determine it more simply, we define a *decoupling onset field* B' where the extrapolated knee in the J-B curve occurs, shown in Figs. 3, 5, and 6. B' is found empirically to be proportional to B_0; therefore, from Eq. (2), the ratio of the decoupling field for aligned and unaligned samples is expected to be given by

$$\frac{B'_{\text{aligned}}}{B'_{\text{unaligned}}} = \frac{\langle D\rangle_{\text{unaligned}}(\lambda_1+\lambda_2)_{\text{unaligned}}}{\langle D\rangle_{\text{aligned}}(\lambda_1+\lambda_2)_{\text{aligned}}}. \tag{3}$$

Substituting typical values of $B'_{\text{unaligned}}$ and $\langle D\rangle_{\text{unaligned}}$ measured for several bulk sintered unaligned YBCO samples,[26] and a $\langle D\rangle_{\text{aligned}}$ of 5 μm (determined from the micrographs of Fig. 2 assuming the magnetic flux is preferentially channeled along the a,b plane), we find from Eq. (3) that $B'(76\text{ K})_{\text{aligned}}$ is about 0.7 mT. *Here we have also assumed λ to be the same for both the aligned and unaligned*

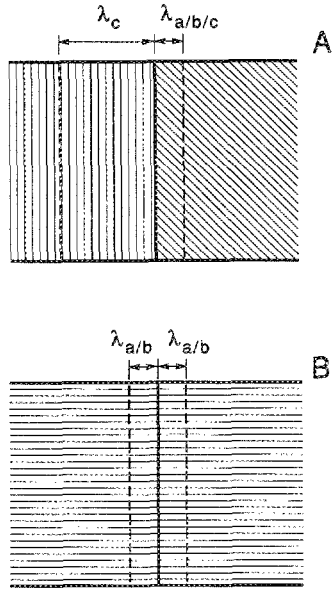

FIG. 10. Schematic of field penetration on either side of a typical grain boundary for (A) unaligned and (B) aligned grain boundaries. Case (A) is typical for unaligned samples since approximately 75% of the grain boundaries in unaligned $Y_1Ba_2Cu_3O_{7-\delta}$ samples have a basal plane face on one side of the grain boundary similar to that shown.

cases. This value of B′ is significantly smaller than the B' of about 2 mT observed in Fig. 3 for both field orientations.

Anisotropy in λ can account for the difference in the decoupling field between the aligned and unaligned case. Micrographic characterization of grain boundaries in unaligned YBCO (Ref. 27) shows that 75% of the grain boundaries involve one grain having a Cu-O basal plane at the boundary with the c-axis perpendicular to the grain boundary; the grain on the other side of such a boundary generally has a random orientation [see Fig. 10(A]. For the grain that has its *c* axis perpendicular to the boundary, the relevant penetration depth for determining B' will be that along the *c* axis, λ_c. λ_c is significantly longer than λ_a or λ_b, as schematically shown in Fig. 10(A). Using the anisotropic effective mass of the YBCO crystal determined in Ref. 28, we find that the ratio of $\lambda_a{:}\lambda_b{:}\lambda_c$ is given by 1.15:1:5.5. For the randomly oriented grain on the other side of the boundary in Fig. 10(A), λ will be mostly dominated by an average of the shorter penetration depths in the *a*- and *b*-axis directions because of the shielding provided by the high conductivity in the Cu-O planes. Thus, as a first approximation for the unaligned case, we take $\lambda_1 = \lambda_c$ and $\lambda_2 = \lambda_a$ (where λ_a has been taken as representative of an *a*/*b* mix to simplify the calculation, since λ_a and λ_b are not very different).

For the aligned YBCO samples being studied here, on the other hand, the penetration depths on either side of the grain boundaries are those along the *a*- and *b*-axes. This is illustrated in Fig. 10(B). For the aligned case, we therefore approximate the penetration depth by $\lambda_1 = \lambda_2 = \lambda_a$, where λ_a has again been taken as representative of an *a*/*b* mix to simplify the calculation. The ratio of $(\lambda_1 + \lambda_2)_{\text{unaligned}}/(\lambda_1 + \lambda_2)_{\text{aligned}}$ in Eq. (3) thus becomes about 2.9 and we obtain from Eq. (3) a value for B' (76 K)$_{\text{aligned}}$ of about 2 mT instead of 0.7 mT obtained using an isotropic λ. Thus, the calculated value of B' is consistent with that measured in Fig. 3, whereas it would not be consistent if the anisotropy of λ in these aligned samples were not taken into consideration.

The decoupling field for the *field-cooled* data in Fig. 6 [B' (76 K) = 4 mT] is about double the decoupling field for the zero-field-cooled data (2 mT). For the zero-field-cooled case, magnetic flux is excluded from the interior of the grains at fields up to the lower critical field B_{c1}. The smallest value of B_{c1} is for field *parallel* to the *a*,*b* plane and has been measured from magnetization data on these samples to be about 3–5 mT at liquid-nitrogen temperature. This is slightly higher than B' and, thus, flux will be compressed at grain boundaries at the low field where decoupling commences. The effect of flux compression will enhance the magnetic field at the grain boundaries for the zero-field-cooled case and thus lower the apparent B'.

For the field-cooled case, on the other hand, flux will uniformly penetrate each grain before cooling below T_c. After cooling, some field will be expelled from each grain, but, because of flux pinning, much of the field will remain within the grain interiors. Not as much flux compression will occur as for the field-cooled care and the onset of decoupling (B') will be delayed to higher fields. Thus, the enhancement of the decoupling field for the field-cooled case over the zero-field-cooled case can be explained by a reduction in the amount of flux compression at the grain boundaries. (This does not affect the *ratio* of B′ values used in the earlier calculation since zero-field-cooled values were used for both the aligned and unaligned cases.)

F. Liquid-helium temperature characteristics

When the transport J_c is measured at lower temperatures in liquid helium, several changes in the characteristics are observed compared with liquid nitrogen temperatures. Comparing Figs. 3 and 5 shows that at 4 K the weak-link decoupling field shifts to higher fields and J_c is enhanced over most of the magnetic-field range. The increase in J_c at higher fields can be accounted for simply in terms of the enhancement in B_{c2}^* and the pinning force that occurs at lower temperatures. The shift in the decoupling onset field B' to higher values can be accounted for, at least in part, by the temperature dependence of λ. λ becomes smaller at lower temperatures, so the junction area decreases and B' increases. The shift of B' to higher values at lower temperature also explains the increase in $J_c(0)$, since a higher self-field can be accommodated before the self-field decouples the superconducting grains in the sample.

The peak in J_c just above the decoupling regime is much less at 4 K than at 76 K, as seen by comparing Figs. 3 and 5. According to the above discussion of the J_c peak, this would indicate that the enhancement of the pinning force just above B_{c1} is not as great at low temperatur e as at liquid nitrogen temperatures.

VII. CONCLUSIONS

Aligned bulk samples of $YBa_2Cu_3O_{7-\delta}$ show weak-link effects at very low magnetic fields ($< 10^{-2}$ T) similar

to unaligned samples. Alignment, however, has two important practical improvements. First, it leads to a significant enhancement in the effective critical field for transport J_c, B^*_{c2}. B^*_{c2} (76 K) is enhanced from about 7 T for unaligned samples to about 30 T for aligned samples with B parallel to the a,b planes. This is very close to the value of B^*_{c2} measured in single crystalline samples for field along the a,b direction, constituting strong evidence that the *inter*granular transport J_c of polycrystalline samples at high fields (>10 mT) is in fact behaving like the *intra*granular J_c and that intrinsic nonweak-linked conduction paths exist in parallel to the weak-linked conduction paths in these polycrystalline samples. This conclusion is also supported by several other observations including: (1) the similarity of the shape of the J_c vs B characteristic above ~ 20 mT to that in single crystalline $Y_1Ba_2Cu_3O_{7-\delta}$ samples, (2) the corresponding anisotropy (with magnetic field angle) of the magnitude of the plateau J_c in these aligned samples to the anisotropy of the transport J_c in single crystalline samples, (3) the strong enhancement of B^*_{c2} at lower temperatures, and (4) a rise in the transition parameter n at magnetic fields above ~ 10 mT, consistent with a transition from a wide distribution of inhomogeneous weak links to a more uniform J_c distribution characteristic of intragranular conduction. There is also evidence for this from neutron irradiation data.[29]

The second result of alignment is a *plateau value of* J_c that is about two orders of magnitude higher than for the unaligned case. That is, there is a significant enhancement in the nearly field-independent value of J_c (which occurs in these bulk-sintered samples in the field region above $\sim 10^{-2}$ T). If this plateau region is ascribed to remnant (nonweak-link) conduction paths, it implies that alignment of grain boundaries results in two orders-of-magnitude increase in the fractional area of nonweak-linked material, compared with unaligned bulk-sintered samples.

The improvement in the plateau J_c cannot be ascribed to the elimination of grain boundaries because these samples are fine grained with many (500–1000) grain boundaries between the voltage-measurement taps. Furthermore, it cannot be ascribed to a large enhancement in the aspect ratio of the grains (wherein the grain boundary area for current transfer between grains is greatly increased). For these samples the grain aspect ratio is only about 4:1, far too small to account for the two orders of magnitude improvement in the plateau value of J_c. These points have been a source of ambiguity in interpreting the enhancement of J_c for melt-grown samples where both alignment as well as elimination and elongation of grain boundaries occur. The data shown here clearly demonstrate that significant improvement in the high-field value of the transport J_c occurs from grain alignment alone.

Regarding the specific nature of the nonweak-linked J_c component, there is some question if it consists of percolation paths connecting a few good grain boundaries, or if some strong linked regions exist within each coherent grain boundary. These data support the latter explanation and are not consistent with percolation paths between a few nonweak-linked grain boundaries. This is because percolative conduction would require at least $\sim 15\%$ of the grain boundaries to be nonweak-linked. Below this percolative threshold, no high-field J_c percolative conduction would occur. Yet our extensive data on both unaligned[1] and these aligned polycrystalline samples show that at least some high-field nonweak-linked transport J_c is observed in nearly all high-T_c samples, inconsistent with a percolative threshold model. The presence of some nonweak-linked transport conduction in such a wide range of samples is much more consistent with the explanation that strong links exist within each grain boundary. Furthermore, as indicated in the introduction, recent J_c data on individual grain boundaries in thin films indicate that the grain boundary structure is very complex. It is thus likely that there are regions of coincidence within each coherent grain boundary which are not weak linked.

Significant further improvement in the areal fraction of nonweak-linked (or strongly linked) grain-boundary material may be possible. Since the nonweak-linked grain boundary material behaves like the intragranular material, it is tempting to assume that the local J_c of the strong links is also similar to J_c for the intragranular material. Assuming a J_c (76 K) of 10^5 A/cm^2 to 10^6 A/cm^2 and that strong links exist *within each* coherent grain boundary, we find from the value of the plateau J_c in these partially aligned samples that the average fraction of grain boundary area that is strongly coupled is still only about 0.01%–0.1% of the total grain-boundary area. (This small areal fraction does not rule out the model. Assuming an areal fraction of 0.01% and an average grain boundary size of 10 μm$\times$10 μm, the nonweak-linked region would still occupy a total area of 10^6 Å^2 within each grain boundary, which is not unreasonably small.) Neutron diffraction data on these samples indicate that the FWHM angular spread of the grain orientations is about 19°, much wider than the $<1°$ angular FWHM typical for high-quality epitaxial film samples. Consequently, significant further optimization may be possible through better grain alignment to the point where conduction by nonweak-linked percolation paths dominates the weak-linked conduction paths.

Such an enhancement of the nonweak-linked component would result in a practical J_c vs B characteristic similar to that in high-quality thin films, where J_c is nearly field independent and not depressed to low values by the application of small magnetic fields. These data thus demonstrate the necessity of grain alignment in bulk $Y_1Ba_2Cu_3O_{7-\delta}$ conductors in order to realize their potential for both low-field and high-field J_c performance.

Other more minor changes between the aligned and unaligned cases include an enhancement by a factor of four in the decoupling field for the aligned polycrystalline samples. This can be explained by the smaller a,b-axis field penetration depth on either side of grain boundaries that are aligned. A peak in the J_c-vs-B characteristic is also observed in aligned samples for field parallel tothe a,b planes. This reversal in J_c with magnetic field occurs in the range between 10 mT and 20 mT. Such a large ($\sim 100\%$ increase) peak at these low fields is not observed in un-

aligned $Y_1Ba_2Cu_3O_{7-\delta}$ samples. There is a significant increase in J_c on cooling from 76 K to 4 K, similar to the unaligned case, which is ascribed to an enhancement of the weak-link decoupling field B_0, the flux- flow pinning force, and the transport critical field B^*_{c2}.

ACKNOWLEDGMENTS

We wish to acknowledge G. Reinacker, T. Larson, and N. Bergren for help in making the critical current measurements, M. J. Curran for help in sample preparation, J. D. Livingston for providing light micrographs of the sample, R. Goldfarb and R. Loughran for making the ac susceptibility and sample density measurements. We also express our appreciation to R. L. Peterson, S. E. Russek, J. Cave, R. B. Goldfarb, and L. F. Goodrich for helpful discussions. JWE gratefully acknowledges the NIST high-T_c program, the Department of Energy/Office of Fusion Energy, and the Office of Naval Research under interagency agreement No. N0001490WM15504 for support for this research. HRH wishes to thank the School of Applied and Engineering Physics of Cornell University for its hospitality during a portion of this work. The high-field experimental data were obtained using the magnet facilities of the Francis Bitter National Magnet Laboratory.

[1] J. W. Ekin, T. M. Larson, A. M. Hermann, Z. Z. Sheng, K. Togano, and H. Kumakura, Physica C **160**, 489 (1989).
[2] H. Dersch and G. Blatter, Phys. Rev. B **38**, 391 (1988).
[3] D. Dimos, P. Chaudhari, and J. Mannhart, Phys. Rev. B **41**, 4038 (1990).
[4] S. Russek and R. Buhrman, *Science and Technology of Thin Film Superconductors 2*, edited by B. McConnell and S. Wolf (Plenum, New York, 1990).
[5] S. E. Babcock and D. C. Larbalestier, Appl. Phys. Lett. **55**, 393 (1989).
[6] T. R. Dinger, T. K. Worthington, W. J. Gallagher, and R. L. Sandstrom, Phys. Rev. Lett. **58**, 2687 (1987).
[7] U. Welp, M. Grimsditch, H. You, W. K. Kwok, M. M. Fang, G. W. Crabtree, and J. Z. Liu, Physica C **161**, 1 (1989).
[8] U. Welp, W. K. Kwok, G. W. Crabtree, K. G. Vandervoort, and J. Z. Liu, submitted to Phys. Rev. Lett. **62**, 1908 (1989). Note that a significantly higher value of the upper critical field is obtained for magnetization, which is associated with the thermodynamic upper critical field; however, the transport critical field, associated with flux flow, is the relevant quantity for consistancy in interpreting the effect of field anisotropy on the transport flux-flow data.
[9] U. Welp, W. K. Kwok, G. W. Crabtree, K. G. Vandervoort, and J. Z. Liu, Phys. Rev. B **40**, 5263 (1989).
[10] D. E. Farrell, M. M. Fang, and N. P. Bansal (unpublished).
[11] J. J. Neumeier, Y. Dalichaouch, R. R. Hake, B. W. Lee, M. B. Maple, M. S. Torikachvili, K. N. Yang, R. P. Guertin, and M. V. Kuric, Physica C **152**, 293 (1988).
[12] R. H. Arendt, A. R. Gaddipati, M. F. Garbauskas, E. L. Hall, H. R. Hart, Jr., K. W. Lay, J. D. Livingston, F. E. Luborsky, and L. L. Schilling, Mater. Res. Soc. Symp. Proc. **99**, 203 (1988).
[13] D. E. Farrell, B. S. Chandrasekhar, M. R. DeGuire, M. M. Fang, V. G. Kogan, J. R. Clem, and D. K. Finnemore, Phys. Rev. B **36**, 4025 (1987).
[14] M. F. Garbauskas, R. H. Arendt, and J. S. Kasper, Inorg. Chem **26**, 3191 (1987).
[15] J. D. Livingston, A. R. Gaddipati, and R. W. Arendt, Mater. Res. Soc. Symp. Proc. **99**, 931 (1988).
[16] D. B. Knorr and J. D. Livingston, Super. Sci. Tech. (in press).
[17] Y. J. Uemura, B. J. Sternlieb, D. E. Cox, V. J. Emery, A. Moodenbaugh, M. Suenaga, J. H. Brewer, J. F. Carolan, W. Hardy, R. Kadono, J. R. Kempton, R. F. Kieff, S. R. Kreitzman, G. M. Luke, P. Mulhern, T. Riseman, D. L. Williams, B. X. Yang, W. J. Kossler, X. H. Yu, H. Schone, C. E. Stronach, J. Gopalakrishnan, M. A. Subramanian, A. W. Sleight, H. Hart, K. W. Lay, H. Takagi, S. Uchida, Y. Hidaka, T. Murakami, S. Etemad, P. Barboux, D. Keane, V. Lee, and D. C. Johnston, J. Phys. (Paris) Colloq. **49**, C8-2087 (1988).
[18] J. W. Ekin, A. J. Panson, and B. A. Blankenship, Appl. Phys. Lett. **52**, 331 (1988).
[19] Y. Tzeng, A. Holt, and R. Ely, Appl. Phys. Lett. **52**, 155 (1988).
[20] J. W. Ekin, A. J. Panson, and B. A. Blankenship, in *High Temperature Superconductors*, edited by M. B. Brodsky, H. L. Tuller, R. C. Dynes, and K. Kitazawa (Materials Research Society, Pittsburgh, PA, 1988), Symposium Proceedings No. 99, pp. 283–286.
[21] J. W. Ekin, T. M. Larson, N. F. Bergren, A. J. Nelson, A. B. Swartzlander, L. L. Kazmerski, A. J. Panson, and B. A. Blankenship, Appl. Phys. Lett. **52**, 1819 (1988).
[22] J. W. Ekin, Appl. Phys. Lett. **55**, 905 (1989).
[23] J. W. Ekin and T. M. Larson, "Dependence of the critical current on angle between magnetic field and current in Y-, Bi-, and Tl-based high-T_c superconductors," presented at the 6th Japan-U.S. Workshop on High-Field Superconductors, Boulder, CO, February 22–24, 1989; *Proceedings of the 6th Japan-U.S. Workshop on High-Field Superconductors and Standard Procedures for High-Field Superconducting Materials Testing*, edited by K. Tachikawa, K. Yamafuji, H. Wada, J. W. Ekin, and M. Suenaga (Sci. Tech. Agency, Japan, 1989), p. 61.
[24] R. J. Loughran and R. B. Goldfarb, H. R. Hart., Jr., and A. R. Goddipati, Bull. Am. Phys. Soc., **35**, 338 (1990).
[25] R. L. Peterson and J. W. Ekin, Phys. Rev. B **37**, 9848 (1988).
[26] R. L. Peterson and J. W. Ekin, Physica C **157**, 325 (1989).
[27] S. Nakahara, G. J. Fisanick, M. F. Yan, R. B. Van Dover, T. Boone, and R. Moore, J. Cryst. Growth **85**, 639 (1987).
[28] G. J. Dolan, F. Holtzberg, C. Feild, and T. R. Dinger, Phys. Rev. Lett. **62**, 2184 (1989).
[29] H. Kupfer, U. Wiech, I. Apfelstedt, R. Flukiger, R. Meier-Hirmer, T. Wolf, and H. Scheurer, IEEE Trans. Magn. **MAG-25**, 2303 (1989).